

# Posture Control in Personal Mobility Robots through Pressure Interfaces

Celine Tchernin, Jorge Peña-Queralta, Yang Chen, Diego Paez-Granados

**Abstract**—Interfaces for shared control of assistive mobility robots are often limited to either joysticks or wearable devices. While recent works have showcased the potential of wearables to promote physical activity, their setup can be cumbersome. This paper explores the potential of non-intrusive methods for controlling robotic wheelchairs, advancing the development of more user-friendly mobility solutions. Using pressure sensors embedded in the wheelchair seat and backrest, our objective is to assess whether a data-based approach can offer advantages over model-based controllers. Our baseline for the model-based controller is the state-of-the-art control methods based on the measured pressure distributions. We compare to this baseline the control performances achieved with data-based approaches. Such methods have the advantage to not require a calibration step. We collected a novel open-source dataset with six different drivers. The dataset, gathered using a commercial pressure mat, can be readily applied to the control of other robotic systems. We successfully demonstrate controllability without the need for wearables or other external systems, paving the way for a zero-shot approach. The dataset and sample code are available at: <https://github.com/tchernin/posture-control>.

**Index Terms**—Shared Autonomy; Control; Personal Mobility; Pressure Control; Dataset

## I. INTRODUCTION

Despite the rapid advances in robotics and AI over the past decade, electric wheelchairs remain largely unchanged in terms of intelligence and control [1]. Multiple studies on the integration of wearable sensors for wheelchair control exist in the literature, from EMG or EEG signals [2], [3], to wearable inertial sensors [4], or fully mechanical solutions [5], [6]. New control interfaces can not only increase the usability of electric wheelchairs, but they can also aid in promoting societal inclusion or health benefits from promoted activity, for example with specific approaches to dancing with wheelchairs [7].

Following the trend toward more active wheelchair interface designs, this study proposes a recreational wheelchair control algorithm that allows users to navigate simply by using their bodies as a joystick. The system is intended for individuals who retain mobility in their upper body.

C. Tchernin is with the InTECH institute, HEPIA, University of Applied Sciences and Arts of Western Switzerland, Geneva, and with the University of Applied Sciences of Eastern Switzerland - OST. J. Peña-Queralta is with the Centre for Artificial Intelligence, Zurich University of Applied Sciences - ZHAW. Y. Chen is with the Laboratory of Intelligent Systems, Swiss Federal Technology Institute of Lausanne -EPFL. D. Paez-Granados is with Swiss Paraplegic Research, SPF, Nottwil. All authors are with the SCAI Lab, D-HEST, Swiss Federal School of Technology in Zurich - ETH Zurich.

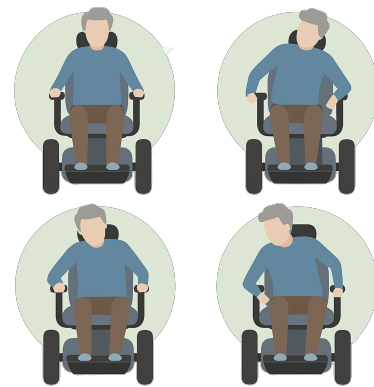


Fig. 1: Conceptual illustration of the proposed approach. Using pressure sensors, the user can control the wheelchair by inclining their body (front, back, sideways or diagonally) without the need for any wearable sensor or calibration step. The movements are exaggerated for illustrative purposes.

While the objective is to provide a new way of controlling the wheelchair for individuals with reduced mobility, only healthy subjects tested the result of this study. If proven effective, such an approach can help to promote physical activity and, for example, reduce the risk of developing pressure injuries due to prolonged periods spent in the same position. This concept is illustrated with sample body positions in Fig. 1.

As a hands-free navigation method, this approach offers a potential alternative to traditional joystick controls, which require manual dexterity and may not be suitable for all users. Additionally, it allows drivers to use their hands for purposes other than navigating the wheelchair, such as playing ball games or other leisure activities.

We develop and compare several pressure-based control methods for wheelchair navigation. These methods differ from existing approaches in two key ways: (i) they are non-intrusive and rely solely on pressure sensor mats integrated into the wheelchair, eliminating the need for wearable or external systems; and (ii) they follow a “sit-and-go” policy—referred to hereafter as “universal”—meaning that no adjustment or calibration is required: the user can simply sit in the wheelchair and begin navigating.

We tested several approaches to better understand which ones merit further development. We began with the center-of-pressure (COP) control algorithm, which requires calibration

and is affected by balance instability caused by the inverted pendulum effect [8]. Due to the system’s dynamic instability, the driver’s center of pressure tends to oscillate unintentionally while the wheelchair is in motion. With COP control, this results in unintended slowdowns during forward movement.

To address this issue, we consider two possible approaches: *i*) developing a physics-based model that accounts for the dynamic interactions between the user, the wheelchair, and the ground, which would then be used to stabilize the COP control algorithm; and *ii*) collecting a dataset with high variability in participants and terrain to train a data-driven model.

The first option seems unrealistic, as a real-world system can hardly be fully captured with simplified physics-based equations, especially when not all physical parameters (such as friction) are known. This approach also limits the usability of the control method to users with specific body morphologies, since the model coefficients are tailored for drivers with specific weight and height. This was the case in [9], which used this approach in the context of trunk-torso COP control.

Those challenges can be mitigated by adopting a data-driven approach, as such models can learn personalized behaviors without relying on explicit equations. If the dataset includes sufficient variability in user morphologies, we may even be able to develop a “universal” control algorithm. Therefore, we decided to investigate the performance of machine learning (ML) algorithms for posture-based control. In particular, we explored the potential of deep neural networks (DNNs).

The main contribution of this work is the design, implementation and comparison of different approaches to pressure-based control, with a focus on exploring the potential of deep learning approaches. While at a proof of concept level, we provide, to the best of our knowledge, the first generalizable end-to-end controller based entirely on pressure sensors and onboard odometry data that does not require user-specific configuration of calibration.

## II. RELATED WORKS

Using upper-body movements to control wheelchair navigation can enhance user well-being by providing a fun, active way to help prevent pressure injuries, while also promoting mental engagement and a positive mood. This approach adds to the range of existing control options that make use of remaining physical abilities and can serve as an alternative to traditional joysticks (see the list in [9] for details). The interfaces listed there are however tailored to people with severe motor disabilities, and who cannot use conventional controls.

Research has explored inferring human pose from pressure sensors. For example, [10] developed an artificial neural network model to infer the 3D human pose from limited pressure information (using the visual dataset as ground truth). This concept was further developed in [11] within the

context of bed-monitoring. In another study, [12] proposed a physics-based model to simulate 3D human poses and shapes at rest, using pressure images as input for a convolutional neural network.

Posture-based control methods have also been explored. For instance, approaches to control self-balancing wheelchairs were developed in [13], [14], [15]. In [16], two IMUs placed on each shoulder were used to detect posture changes and map them into wheelchair control commands.

In [6], the authors developed a steering-by-leaning system that controls the wheelchair’s front wheels. Meanwhile, [7] used machine learning classifiers for recognizing wheelchair dance gestures, based on data from two six-axis IMUs placed on the driver’s hands. However, the development of a wheelchair control interface based on these dance gestures is still lacking. A dancing wheelchair, which enhances mobility, was also developed in [17]. In another study closer to the present work, the changes in a rider’s posture were detected with pressure mats attached to the seat and backrest of the wheelchair ([18]). Their goal was to control the left/right turning intention with pressure data, while forward/backward motions were controlled with switches located on the feet. We note that a thorough assessment of this left/right control method has not been published yet. Focusing on upper-body able users, [19] developed a control interface with natural body motions of the torso. This method is based on the center of pressure computed along a one-dimensional Force-sensing resistor (FSR) array. The movement control of the robot is then determined using a continuous function of the pressure magnitude and the COP. Combining IMU with pressure sensors, as a further development of the work done in [19], [9] designed a torso-based control interface with a coupling support that improves the stability of the driving experience using a model that accounts for the undesirable dynamic effects (due to the inverse pendulum effect). The implementation of this correction into the controller design is however still lacking.

## III. DATASET DESCRIPTION

For data collection, we established a protocol in which each participant was asked to navigate specific circuit shapes using the wheelchair joystick (mounted on the right side of the wheelchair), while simultaneously mimicking the posture changes they would use to control the wheelchair with their body. The recorded joystick values serve as ground truth for training the machine learning algorithm.

Our data collection protocol consists of well-defined circuit shapes (see Table I): a rectangle driven in both directions (*Rect*), a rotation in place (*Rotating*), and a forward motion with braking (*Move-stop*). For further analysis, we also collected data for the less structured patterns: random motion (*Random*), figure-eight shape (*Eight*) and acceleration (*Acc*). Each experiment was repeated under two different dynamic settings: level speed 1 (which corresponds to 0.3 m/s) and

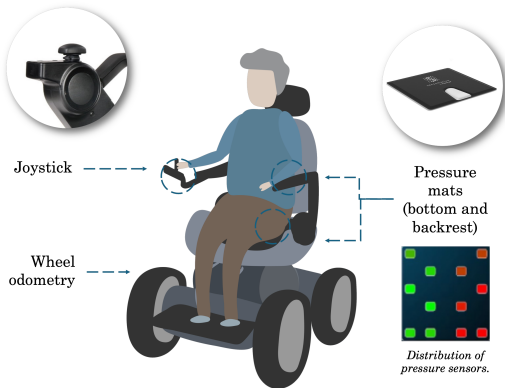


Fig. 2: Experimental setup illustration, with representation of the position of the pressure mats and other sensors on the wheelchair. Bottom right: graphical representation of the distribution of the sensors on the *Sensomative* pressure mat.

TABLE I: Dataset: number of samples collected per circuit shape, for the two dynamical settings: speed level 1 and 3. The data were extracted from the recordings at 10Hz.

	Rect	Eight	Acc	Rand.	Rot.	Move-stop	Total
User1	3313	1145	123	816	554	568	6519
User2	3450	1511	424	1075	603	594	7657
User3	1396	1084	276	860	564	587	4767
User4	3531	1529	0	2266	791	706	8823
User5	3719	1400	343	1277	560	527	7826
User6	3037	1355	288	1381	634	613	7308
<b>Total</b>	<b>18446</b>	<b>8024</b>	<b>1454</b>	<b>7675</b>	<b>3706</b>	<b>3595</b>	<b>42900</b>

level speed 3 (which corresponds to 1.1 m/s). A summary of the datasets collected for each circuit shape and speed setting is provided in Table I. Six participants were involved in the data collection.

#### A. Data Collection

We use the *Sensomative wheelchair* pressure mats from the company Sensomative [20]. Each mat contains 12 sensors, whose distribution is shown in Fig. 2. As seen in the figure, the sensor layout is symmetric between the left and right sides, but asymmetric between the front and the back sections of the mat. Two mats have been used: one placed on the seat (on top of the wheelchair cushion) and one on the backrest.

The sensor modalities used during data collection are listed in Table II.

We consider two analysis frameworks: classification and regression. For the classification tasks, we consider four mutually exclusive classes: *Fw*, *S*, *L*, and *R*. This requires careful data cleaning, where all transition periods and any time steps during which both joystick axes were simultaneously active must be removed. Due to the variety of behavior of our six participants, we needed to define different thresholds for each user at each dynamical set-ups (speed level 1 and 3). The fraction of the removed data was nevertheless

TABLE II: Table of sensors: Sensor modalities and data recording frequencies. SW stands for Sensomative Wheelchair, MM for MbientLab MetaMotionS. In the case of the DNN approaches, the entry *Usage* specifies whether the sensor is being used as inference (*I*) or ground truth (*GT*). The entry *methods* outlines the methods in which the dataset is being used: *A* stands for COP; *B*, Neural network for classification; and *C*, Neural network for end-to-end regression. The rosbags where these data are being recorded are available in <https://github.com/tchernin/posture-control/tree/master/data>.

Modality	Sensor	Location	Frequency [Hz]	Dimensionality Usage, Methods
<b>Pressure</b>	SW	Seat	10	12, I, A, B, C
<b>Pressure</b>	SW	Backrest	10	12, I, C
<b>Odomet</b>	Odometry	Internal	20	2, I, C
<b>Joy</b>	Joystick	Right hand	20	2, GT, B, C

reasonably small (about 12%). In this analysis, we used the circuit shapes: *Rect*; *Rotating*, and *Move-stop* (referred as *the structured circuit shapes*). For the regression tasks, we consider the raw data. While we tested our algorithm on any circuit shape, we used only the structured circuits shapes for training.

## IV. METHODOLOGY

In this section, we describe the methods investigated for controlling the wheelchair based on the user's posture changes. We begin with the Center of Pressure (COP) method, followed by the Deep Neural Network (DNN) models tested for both user intention detection (classification tasks) and end-to-end hands-free wheelchair control (regression tasks).

The study was carried out using the WHILL Model C2 wheelchair<sup>1</sup>, a non-holonomic system. The control is limited to a subspace involving forward, left, and right movements. We intentionally limited backward drive for safety concerns.

#### A. Center of Pressure (COP): Model-Based Controller

The center-of-pressure (COP) control algorithm is straightforward to implement and set up. However, it requires a calibration step.

We extend the COP-based approach proposed in [19] from one to two dimensions: the location of the COP now spans a plane, which is similar to the space spanned by the joystick. Formula 1 from [19] is adapted as follows:

$$COP_{\eta} = \frac{\sum_1^n w_i p_i \eta_i}{\sum_1^n p_i} - COP_{\eta 0}. \quad (1)$$

Where  $\eta$  stands for  $x$  or  $y$ , while  $w_i$  represents the weight of the sensor  $i$  ( $i$  from 1 to  $n=12$ , for the 12 pressure sensors placed on the mat, bottom-right representation in Fig. 2). The values of these weights were set by taking the average of the

<sup>1</sup><https://whill.inc/us/whill-model-c2/>

10 maximum sensor values reached by each sensor during the calibration phase. Then,  $p_i$  corresponds to the current measurement value of the sensor  $i$  and  $x_i$  ( $y_i$ ), to the position of the sensor  $i$  on the pressure mat along the x (y) axis. A representation of the spatial distribution of the sensors on the pressure mat is shown in Fig. 2. Finally, the quantities  $COP_{x0}$  and  $COP_{y0}$  are determined during the calibration phase. They correspond to the neutral position of the driver, indicating that the driver is relaxing and does not intend to move. In the following, these values will be called the “COP 0-value”. As a sanity check, we verified that the pressure read at the sensor is a linear function of the force applied. This ensures that the pressure measurement  $p_i$  can be used directly in these equations without further transformation. This COP computation serves as our baseline model for our analysis.

### B. Intent Classification: Data-Based Approach

We aim to detect user intention based on pressure distribution measured on the wheelchair seat. We use a fully connected multilayer perceptron (MLP) with six hidden layers, ending in a 4-unit output layer corresponding to the intention classes: moving forward (Fw), stopping (S), turning left (L), and turning right (R).

Due to class imbalance—particularly the overrepresentation of the Fw class—we evaluate performance using the F1-score. We tested the model using various combinations of input features: seat pressure alone; past odometry values (up to 0.2 and 0.6 seconds); and differential pressure computed over a 0.3-second time lag. Note that the hyperparameter grid search was conducted using only seat pressure as input. Results are reported in Section V-A.

### C. Intent Regression: Data-Based Approach

We use the raw data described in Section III to train a model that predicts joystick axis values. The input features include pressure readings from both the seat and back mats, as well as odometry measurements capturing the wheelchair’s motion. The model is a multilayer perceptron (MLP) with six hidden layers and a 2-unit output layer. Implementation and training details are available on our GitHub page. To ensure the model produces zero output in the absence of input, artificial zero-valued samples were included in the training set but excluded from the validation set. We evaluated various input configurations, including pressure (seat and back), odometry, differential pressure across past time steps, and past odometry values (up to 0.6 seconds). We evaluated the performances of this algorithm in term of MSE loss.

We tested several combinations of the input data: pressure (seat+back); odometry; differential pressure (for the different time steps in the past); odometry values in the past (up to 0.6 seconds).

### D. Setup for the Qualitative Assessment

The qualitative assessment involved ten participants who were not part of the training data collection. Each participant

evaluated five control models in a structured procedure. For each model, participants first familiarized themselves with the control algorithm by performing predefined movements—tracing a rectangle, a figure-eight, and then moving freely—first with arms in their preferred position, then with arms extended. Once participants were comfortable using the control algorithm, they exited the wheelchair and completed a questionnaire to evaluate it. These steps were repeated for each model. Based on individual preferences and reactions, the selection of subsequent models was occasionally adapted.

To ensure consistency across evaluations, the first model tested was repeated during the assessment, resulting in four models evaluated for each participant. Model identities were concealed to prevent bias. To enable comparison across participants, individual questionnaire scores were rescaled to a [0, 1] range based on each participant’s own minimum and maximum ratings.

## V. EXPERIMENTAL RESULTS

### A. Intent Classification:

1) *Model-Based Controller*: We use the COP algorithm to classify between the four following users intentions: move forward ( $Fw$ ), brake/stop ( $S$ ), turn left ( $L$ ) and turn right ( $R$ ).

The performances achieved with the COP predictions can be evaluated both in terms of the driver intention classification and in terms of end-to-end posture-based control. It is important to note that only real-time measured pressure values are utilized in this control scheme. The following procedure is adopted to enable offline use and perform classification tasks:

- To replace the calibration step, we derive the COP 0-value for each user from the clean data labeled with the intention “Stop”.
- For each axis, the continuous COP value is converted into a class by using a threshold.

2) *Data-Based Approach*: We trained the neural network using different input combinations, focusing on seat pressure and odometry data to fairly compare with the COP method (excluding the back pressure mat). Input variables tested include raw pressure (P), differential pressure with a 0.3-second lag (D), odometry (O), and odometry delayed by up to 0.2 seconds (V2) and 0.6 seconds (V6), capturing past dynamic information. We evaluated the model using three validation procedures: 30% holdout, leave-one-user-out (LOOCV), and leave-one-shape-of-one-user-out. We report here the results for the LOOCV validation method. Results for the other validation methods are omitted but are available in the extended analysis upon request to the authors.

3) *Comparison Model-Based Controller vs Data-Based Approach*: The F1-score performances from the offline analysis, per class and per user, are shown in Fig. 3 and Table III. The four classes are, from top to bottom and left to right: moving forward, turning left, stopping and turning right. The F1-score obtained from the COP method is shown in blue, with the solid line indicating the median and the shaded

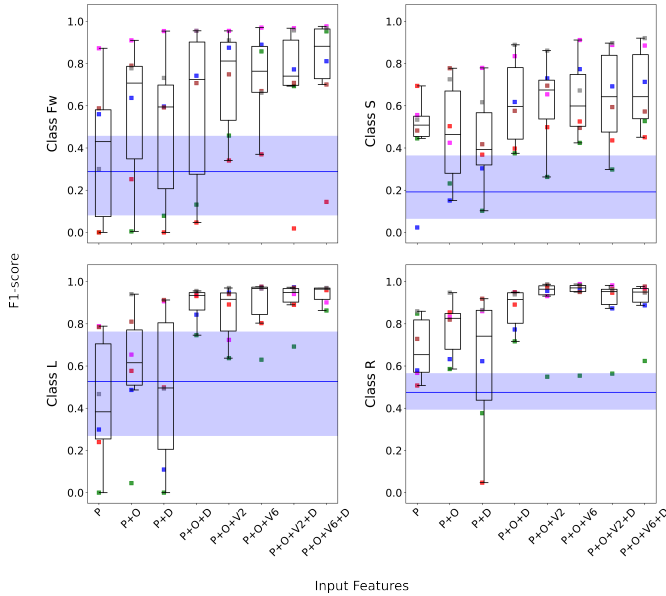


Fig. 3: Comparison of User Intention Classification and COP Model Performance. F1-score performance per user and per class is shown for various input feature combinations used in the data-driven classification approach (evaluated using leave-one-out cross-validation, LOOCV). These results are overlaid on the COP model outcomes for direct comparison. Separate panels display results for each class. Input features are: "P": seat pressure, "D": differential pressure (0.3-second lag), "O": odometry, "V2": odometry delayed by up to 0.2 seconds, "V6": odometry delayed by up to 0.6 seconds. See text for further details. Corresponding values are listed in Tab. III.)

area representing the interquartile range (from the first to the third quartile) across the six users who participated in the data collection. The LOOCV F1-score performance is presented per class and per user for the selected input feature combinations. Colored points represent individual users, while black boxplots illustrate the distribution of F1-scores across the six users.

TABLE III: Intention recognition performance for each tested method, reported per class, with F1-score (F1), balanced accuracy (BA) across all classes. This table presents a selection of the MLP best-performing models from Fig. 3.

Method	BA Mean $\pm$ Std	Class	F1 Mean $\pm$ Std
COP	0.57 $\pm$ 0.07	Fw	0.27 $\pm$ 0.22
		S	0.21 $\pm$ 0.16
		L	0.52 $\pm$ 0.27
		R	0.50 $\pm$ 0.13
MLP: P+O+V6	0.83 $\pm$ 0.10	Fw	0.73 $\pm$ 0.20
		S	0.63 $\pm$ 0.17
		L	0.89 $\pm$ 0.13
		R	<b>0.90<math>\pm</math>0.16</b>
MLP: P+O+V6+D	<b>0.85<math>\pm</math>0.07</b>	Fw	<b>0.76<math>\pm</math>0.29</b>
		S	<b>0.68<math>\pm</math>0.18</b>
		L	<b>0.94<math>\pm</math>0.04</b>
		R	0.89 $\pm$ 0.12

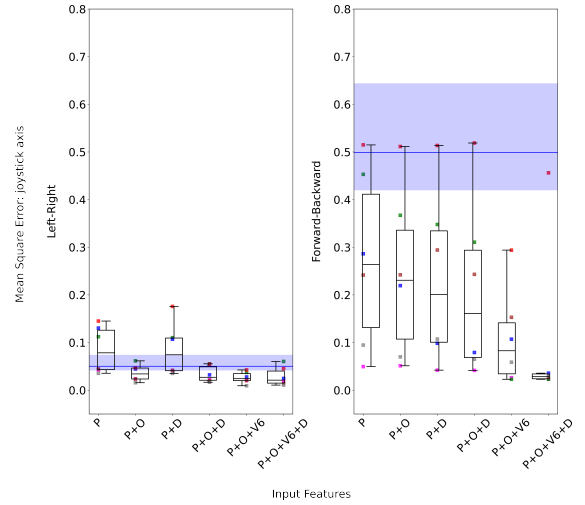


Fig. 4: Comparison of User Intention Regression and COP Model Performance. MSE for both joystick axes is shown across various input feature combinations used in the data-driven regression approach (evaluated using LOOCV). Results are overlaid with COP model outcomes for direct comparison. Left: joystick axis for left/right motion; right: axis for forward/backward motion.

### B. Intent Regression: Offline Evaluation

We evaluate the performance of these algorithms in both offline and real-time setups. We report first the offline results.

1) *Model-Based Controller*: The two-dimensional COP predictions are directly compared to the joystick ground truth. The calibration step is performed similarly to that in the classification task.

2) *Data-Based Approach*: We trained the neural network using the same input feature combinations as in the classification task, except for V2, which was excluded. For this task, both pressure mats—on the seat and the backrest—were used.

3) *Comparison Model-Based Controller vs Data-Based Approach*: The MSE performance for the multi-output regression are presented in Fig. 4 and in Table IV. Predictions for the joystick axes—left/right and stop/forward—are shown in the left and right panels, respectively. The COP predictions are directly compared with those obtained using trained neural networks with various combinations of input features. The MSE loss from the COP method is shown in blue, with the solid line for the median and the shaded area representing the range from the first to the third quartile among the six users. Colored points represent the results from the data-driven approach using LOOCV validation; the MSE loss for each user is represented by a unique color, while black boxplots illustrate the distribution of MSE loss across the six users.

### C. Intent Regression: Real-Time Evaluation

Our main findings from the qualitative assessment (QA) are presented in Fig. 5. The corresponding questions relate to safety, reliability, and user satisfaction. In this figure,

TABLE IV: User intention regression performance per method and control command (joystick axis), with best-performing MLP models selected from Fig. 4

Method	Control command	MSE Mean $\pm$ Std
COP	L/R	0.06 $\pm$ 0.03
	Fw/S	0.53 $\pm$ 0.13
MLP: P+O+V6	L/R	<b>0.03<math>\pm</math>0.01</b>
	Fw/S	0.11 $\pm$ 0.09
MLP: P+O+V6+D	L/R	0.03 $\pm$ 0.02
	Fw/S	<b>0.10<math>\pm</math>0.12</b>

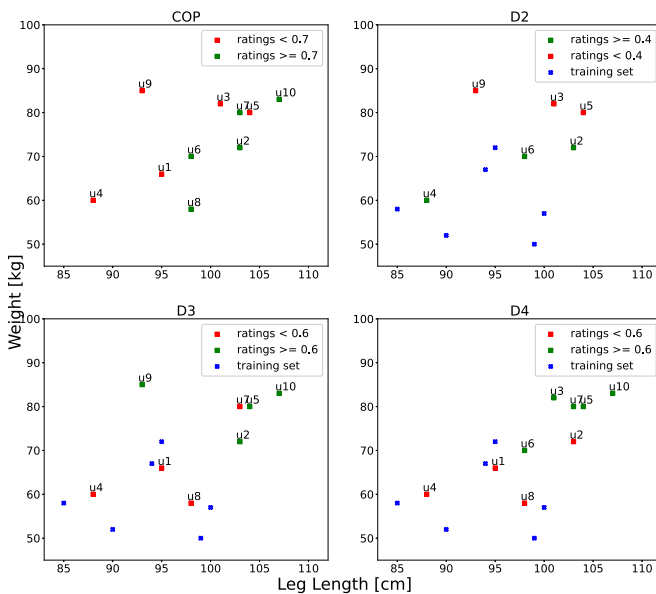


Fig. 5: Ratings per model for questions on reliability, safety, and satisfaction, shown alongside participants’ body dimensions. Red and green indicate ratings below and above the median, respectively; blue shows the users’ body dimensions from the training set. Models are arranged top to bottom, left to right: COP, followed by MLP models trained on P+D2+O, P+D3+O, and P+D4+O inputs. Credits: Celine Tchernin Master’s Thesis.

we explore whether the ratings given by participants for each algorithm are influenced by their physical morphology. Specifically, we compare participants’ weight and leg length to the ratings they assigned to the different models.

We present results for the following models: COP, D2, D3, and D4. These MLP models use the input feature set “P + O + Di,” where P is pressure data (seat and backrest), O is odometry, and Di represents differential pressure computed over  $0.1 \times i$  seconds in the past. The figure’s color scale highlights ratings relative to the median—red indicates below-median ratings, green indicates above-median. Body dimensions of the six participants are shown in blue. For completeness, the figure also includes the median rating for each model across all questions.

## VI. DISCUSSION & CONCLUSION

We investigated posture-based wheelchair control using a 12-sensor pressure mat (Sensomative, Switzerland), exploring whether a “universal” model—requiring no per-user calibration—can robustly infer control commands and handle oscillatory shifts from inverted pendulum effects.

We compared a data-driven approach with a model-based COP baseline for both intent classification and regression tasks. The COP controller, relying solely on real-time seat pressure and a static calibration at rest, fails to account for motion-induced dynamics. In contrast, neural network models using time-delayed odometry (e.g., V2, V6) and differential pressure (D) outperform COP across users and control tasks (Fig. 3, 4), demonstrating the importance of capturing temporal context. Nevertheless, even with a data driven approach, the forward/backward control (joystick axis 2) remains the most challenging task (Fig. 4).

To better understand individual differences in usability, we examined user ratings and morphological data. While COP ratings show no clear correlation with participant morphology (Fig. 5), qualitative feedback indicates that factors such as weight, posture, and seating position can affect control performance. Interestingly, neural models—particularly D2—exhibit a notable negative correlation with participant weight ( $\rho_{D2} = -0.7$ ), a trend that reverses in D3 and D4 ( $\rho_{D3} = 0.5$ ,  $\rho_{D4} = 0.8$ ). These trends suggest that model performance depends on selecting appropriate temporal features, which may vary with user morphology. This highlights the need for architectures—such as LSTM—that can implicitly learn or adapt to these time dependencies based on the user’s body dynamics. We note that the implemented COP algorithm was also successfully tested and demonstrated with young and elderly individuals at Swiss Robotics Day 2023 and at the National Center for Geriatrics and Gerontology (NCGG) in Nagoya, Japan. Demonstration videos are available on our GitHub page.

The evaluation metrics used in this study (MSE and F1-score) were selected primarily as a proof of concept. In future work, we will evaluate the method more thoroughly by measuring reaction time and control responsiveness during predefined movement trajectories, allowing us to assess how well users control the system in realistic conditions.

One key limitation of this study is that the training set, composed of data from six users, does not cover a sufficiently wide range of body types, particularly in terms of height and weight. We expect that a broader data collection including greater morphological variability will improve the generalization and robustness of the trained models. These findings support the idea that expanding the dataset could enable the development of a “universal” model, by capturing a wider spectrum of user characteristics and behaviors. Such a model would be better equipped to generalize across diverse populations, reducing the need for individual calibration and improving overall system adaptability.

#### ACKNOWLEDGMENT

This research work was partially supported by the JST Moonshot R&D (Grant Number JPMJMS2034-18). We would like to thank all the people at ETHZ that have supported this study, took part in the collection of data and in the qualitative assessment experiments. We would like to thank Ostschweizer Fachhochschule (RJ) for allowing CT to pursue this analysis as part of her Master's thesis.

#### REFERENCES

- [1] S. K. Sahoo et al. A review on smart robotic wheelchairs with advancing mobility and independence for individuals with disabilities. *Journal of Decision Analytics and Intelligent Computing*, 3(1):221–242, 2023.
- [2] H. Seki et al. *A powered wheelchair controlled by EMG signals from neck muscles*. Elsevier Science, 2001.
- [3] M. R. Williams et al. Evaluation of head orientation and neck muscle emg signals as three-dimensional command sources. *Journal of NeuroEngineering and Rehabilitation*, 12(1):25, 2015.
- [4] L. Rum et al. Wearable sensors in sports for persons with disability: A systematic review. *Sensors*, 21(5):1858, 2021.
- [5] N. Sebkhi et al. Technical validation of kinemo, a wearable alternative controller for smart control and power wheelchair driving. In *Assistive Technology*, volume 36, pages 84–84, 2024.
- [6] R. Togni et al. Steering-by-leaning facilitates intuitive movement control and improved efficiency in manual wheelchairs. *Journal of NeuroEngineering and Rehabilitation*, 20(1), 2023.
- [7] J. M. Rocha et al. Dance gestures recognition for wheelchair control. In *IEEE ICCRE*, 2023.
- [8] O. Boubaker. The inverted pendulum benchmark in nonlinear control theory: A survey. *Int. J. of Advanced Robotic Systems*, 2013.
- [9] Y. Chen et al. Torso-based control interface for standing mobility-assistive devices. *IEEE/ASME Transactions on Mechatronics*, pages 1–12, 2024.
- [10] Y. Luo. Intelligent carpet: Inferring 3d human pose from tactile signals. In *IEEE/CVF CVPR*, 2021.
- [11] L. Casas et al. Human pose estimation from pressure sensor data. In *Bildverarbeitung für die Medizin 2018*, 2018.
- [12] H. M. Clever et al. Bodies at rest: 3d human pose and shape estimation from a pressure image using synthetic data. In *IEEE/CVF CVPR*, 2020.
- [13] Chronus Robotics. KIM1, 2023. [Online; accessed 1st-June-2024].
- [14] Ltd. Honda Motor Co. Uni-one, 2023. [Online; accessed 1st-June-2024].
- [15] S. Y. Song et al. Design and validation of a torso-dynamics estimation system (tes) for hands-free physical human-robot interaction. In *2023 32nd IEEE International Conference on Robot and Human Interactive Communication (RO-MAN)*, pages 171–178, 2023.
- [16] E. B. Thorp et al. Upper body-based power wheelchair control interface for individuals with tetraplegia. *IEEE Transactions on Neural Systems and Rehabilitation Engineering*, 2016.
- [17] J. C. Luna et al. Volting, a novel dancing wheelchair with augmented mobility: Pushing lateral inclinations. In *IEEE ICORR*, 2023.
- [18] Y. Wakita et al. Riding type vehicle and method of controlling riding type vehicle, 2012. US Patent 8,340,869.
- [19] Y. Chen et al. Control interface for hands-free navigation of standing mobility vehicles based on upper-body natural movements. *IROS*, 2020.
- [20] M. Hubli et al. Feedback improves compliance of pressure relief activities in wheelchair users with spinal cord injury. *Spinal Cord*, 59(2):175–184, 2021.